



A spontaneously formed and self-adjuvanted hydrogel vaccine triggers strong immune responses



Tao He^a, Xiuqi Liang^a, Lu Li^a, Songlin Gong^a, Xinchao Li^a, Miaomiao Zhang^a, Shun Yao Zhu^a, Haitao Xiao^b, Qinjie Wu^{a,*}, Changyang Gong^{a,*}

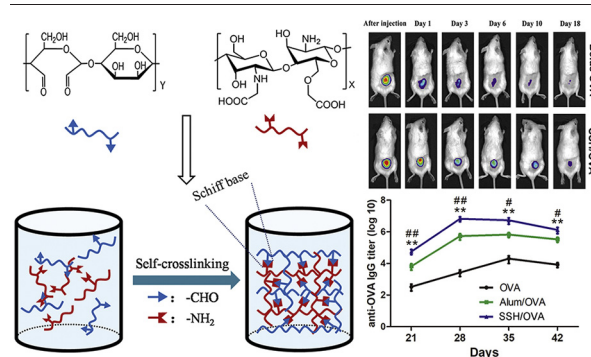
^a State Key Laboratory of Biotherapy and Cancer Center, West China Hospital, Sichuan University, Chengdu 610041, PR China

^b Department of burn and plastic surgery, West China Hospital, Sichuan University, Chengdu 610041, PR China

HIGHLIGHTS

- Novel aldehyde mannan and *N*, *O*-carboxymethyl chitosan based spontaneously formed hydrogel was prepared.
- The hydrogel had both adjuvant potential and the ability to sustained release antigen.
- The hydrogel-based vaccine induced strong antigen-specific immune response without any other immunoadjuvant.

GRAPHICAL ABSTRACT



ARTICLE INFO

Article history:

Received 5 July 2020

Received in revised form 8 September 2020

Accepted 11 October 2020

Available online 14 October 2020

Keywords:

Hydrogel

Spontaneously formed

Self-adjuvant

Vaccine

Immunotherapy

ABSTRACT

Hydrogel is a promising vaccine delivery vehicle, and have been applied to deliver antigens and adjuvants to enhance the immunogenicity of antigens. However, the complexity of hydrogel design, and the high cost and safety hazards of immunostimulating adjuvants have prevented the widespread applications of hydrogel vaccine. In this study, we developed a spontaneously formed and self-adjuvanted hydrogel (SSH) which had both adjuvant potential and the ability to sustained release antigen in situ. Unlike conventional hydrogel vaccine, our SSH was formed without requirement of radiant light sources or any crosslinking initiators. The adjuvant potency of hydrogel was evaluated and results confirmed that hydrogel promoted antigen uptake by dendritic cells (DCs) and induced DCs maturation. Moreover, SSH loaded with ovalbumin increased the accumulation of antigens in lymph nodes. Finally, subcutaneous administration of SSH-based vaccine increased antigen-specific IgG production by 12.5-fold compared with the clinically used aluminum, and delayed tumor growth in vivo. Thus, easily manufactured SSH may serve as a new and powerful antigen delivery platform with immune-stimulating capabilities to promote antitumor immune responses, and has great potential for immunotherapy against different diseases.

© 2020 The Authors. Published by Elsevier Ltd. This is an open access article under the CC BY-NC-ND license (<http://creativecommons.org/licenses/by-nc-nd/4.0/>).

Abbreviations: A-MA, aldehyde mannan NOCC; DC, dendritic cell; OVA, ovalbumin; MTT, 3-(4,5-dimethylthiazol-2-yl)-2,5-diphenyl-tetrazolium bromide; XRD, X-ray diffraction; GPC, gel permeation chromatography; Alum, Aluminum; OVA-FITC, Fluorescein isothiocyanate labeled ovalbumin; OVA-RBITC, Rhodamin B isothiocyanate labeled ovalbumin; SEM, scanning electron microscopy; ESR, equilibrium swelling rate; APC, antigen-presenting cell; ELISA, enzyme-linked immuno sorbent assay.

* Corresponding authors.

E-mail addresses: cellwqj@163.com (Q. Wu), chyong14@163.com (C. Gong).

1. Introduction

Improving the immunogenicity of subunit vaccines is crucial for finding new vaccines against varieties of viral and bacterial infections as well as for designing anticancer vaccines [1–3]. In recent years, various adjuvants have been developed to enhance the immunogenicity of antigens. In compliance with different mechanisms of action, they are

mainly divided into immunostimulatory agents such as Toll-like receptor agonists [4], STING agonists [5] and etc., and antigen delivery systems, such as polymeric nanoparticles [6], three-dimensional scaffolds [7], hydrogels [8] and etc. However, the ideal adjuvant should have a dual action of immunostimulation and antigen delivery [9]. Although the majority of adjuvants combination with antigen could activate an effective immune response compared with free antigens, some obstacles concerning self-immunogenicity, biosafety, and degradability need to be surmounted [10,11]. Therefore, it remains challenging to develop safer and more efficient vaccine adjuvants that can be functioned as both immunostimulatory agents and antigen delivery systems.

Hydrogel is defined as a three-dimensional polymeric network that can imbibe large amount of water [12]. As a vaccine carrier, hydrogel can be used to alter the release kinetics of antigens and immunostimulatory adjuvants and maintain their native configuration, thereby improving the effectiveness of these molecules relative to bolus injection [13]. The large biomolecules loading and controlled release capability as well as distinct degradation profiles of hydrogels render them promising

candidates for immunotherapy of cancer. However, the application of hydrogels in immunotherapy still faces challenges. Hydrogel formation usually requires certain triggers that do not exist in the vaccination environment such as ultraviolet radiation, temperature, enzymes, etc., and additional ultraviolet light and heating are associated with side effects [14–16]. In addition, hydrogels are generally used as a delivery vehicle for antigens or immunostimulatory adjuvants. However, the high cost and unproven safety hazards of many immunostimulant adjuvants hinder their widespread application [17,18]. Thus, in situ injectable hydrogels without cross-linking initiation conditions, especially those with adjuvant function, are very promising vaccine adjuvants.

The use of natural polymers, especially polysaccharides to synthesize hydrogels has attracted considerable attention from researchers. Polysaccharides are more stable, biocompatible, and biodegradable in nature [19]. The biodegradable properties are particularly useful for delivering cargos in a controlled manner locally. Many polysaccharides have chemically active functional groups such as amino, carboxyl and hydroxyl groups, and these groups can be applied for further

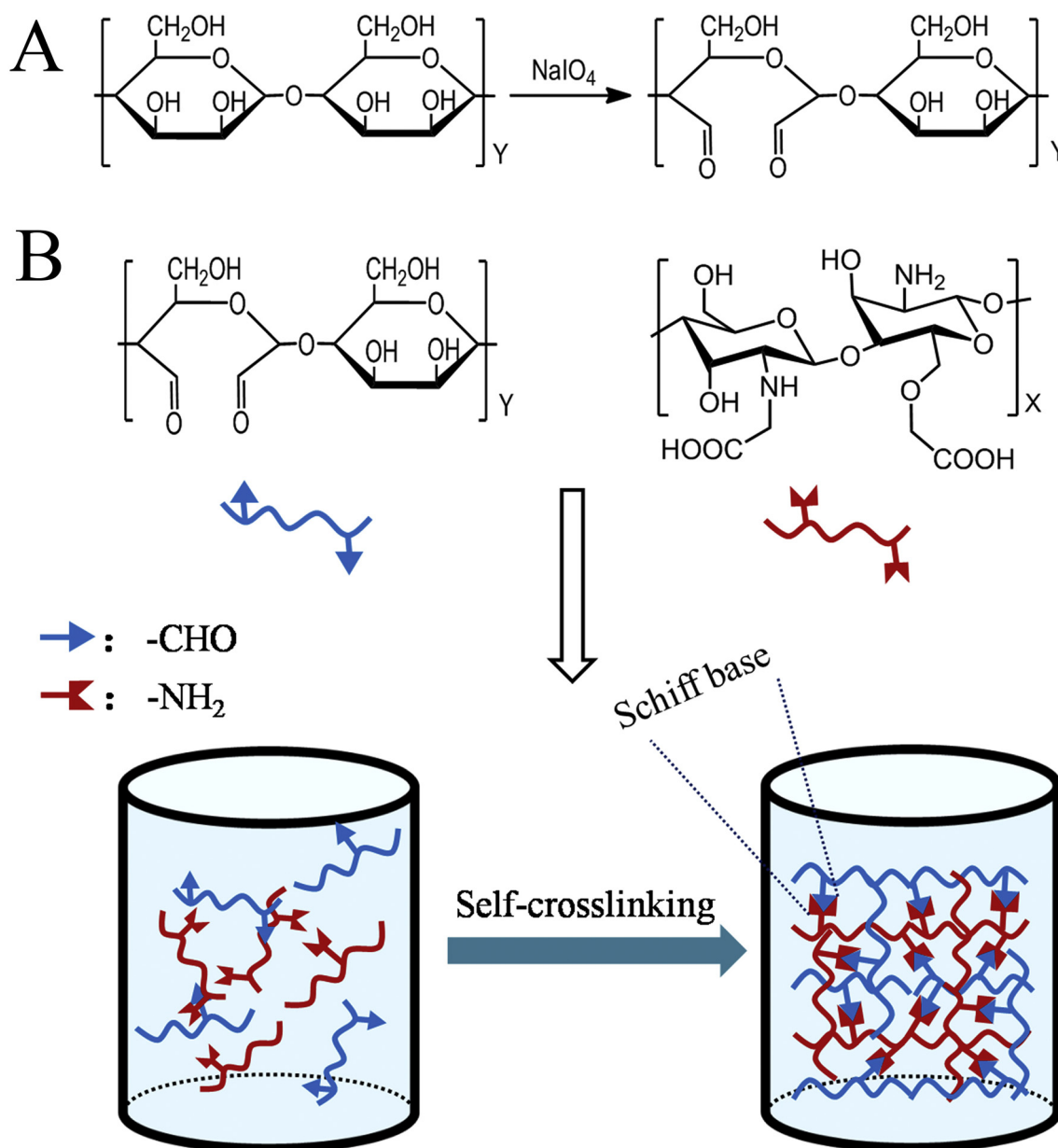


Fig. 1. Synthesis of A-MA and SSH. (A) Synthesis of A-MA; (B) Schematic illustration of the preparation of SSH by cross-linking A-MA with NOCC.

modification in the preparation of controlled release carriers [20]. In addition, monosaccharides, as the monomer units of polysaccharides, have been pointed out by a large and growing amount of information for their key roles in cell signal transduction schemes, especially in the field of immune recognition [21]. Thus, easily modified polysaccharides with immunological activity make it possible to prepare a hydrogel that integrates both antigen sustained release ability and self-adjutant functions.

Mannan is a natural polysaccharide composed of mannose and glucose [22]. Mannose has been shown to be essential in DCs uptake, processing, presentation, thus stimulating downstream immune responses via the mannose receptor [23–25]. Specifically, peptides chemically linked to mannan have been shown to induce potent antigen-specific immunity [26], but complex chemical linkages have limited their further application. Physical encapsulation of proteins to mannan-based hydrogels may be a more convenient and powerful way to elicit strong immune responses. After oxidation by sodium periodate, mannan can cross-link with chitosan to form hydrogels [22]. However, the poor solubility of chitosan in neutral solvents limits its application as an injectable hydrogel. To solve this problem, *N*, *O*-carboxymethyl chitosan (NOCC), a water-soluble chitosan derivative, was synthesized via introducing carboxymethyl groups to the *N*-position and *O*-position of chitosan [27]. Moreover, NOCC has been applied in biomedical field owing to its non-toxicity, biodegradability and non-immunogenic [27–29]. We hypothesize hydrogel based on aldehyde mannan (A-MA) and NOCC could serve as self-adjutant to maintain antigen release to stimulate strong antigen specific immune response without additional immunomodulators.

In this work, a spontaneously formed and self-adjuvanted hydrogel (SSH) derived from A-MA and NOCC were developed. The gelation of SSH is attributed to the formation of Schiff base without additional light sources or any crosslinking initiators. The prepared hydrogel allowed model antigen ovalbumin (OVA) to be incorporated through simple mixing, and then its morphology, rheological properties and degradation were investigated. In addition, we demonstrate the ability of SSH to serve as both immunostimulatory adjuvant and antigen delivery vehicle, and assessed antigen-specific immune responses.

2. Results and discussion

2.1. Preparation and characterization of SSH

Vicinal hydroxyl groups in mannan can be oxidized by NaIO_4 to form dialdehyde derivatives (Fig. 1A). The actual oxidation degree was measured using method of hydroxylamine hydrochloride, and results are shown in Table S1. The structure of A-MA was confirmed by FTIR. As shown in Fig. S1A, similar to previous studies [30], we did not detect the absorption peak of aldehyde group, probably because the hydroxyl and aldehyde groups formed hemiacetal structures.

The diffractograms of A-MA, NOCC and SSH were presented in Fig. S1B. A-MA exhibited signs of being amorphous, and no characteristic peaks were detected. As to NOCC, it exhibited one peak at 17.8° . However, when SSH was formed, two new characteristic diffraction peaks at 31.9° and 45.6° were observed. This may be explained that the formation of Schiff base between $-\text{NH}_2$ of NOCC and $-\text{CHO}$ of A-MA suppresses the crystallization of NOCC. More than that, the peak intensity of hydrogel decreases with the increase of oxidation degree of A-MA (Fig. S1C). As is known, hydrogen bonds between hydroxyl groups and amino groups are key factors to stabilize the crystal structure of chitosan [22]. It may be explained by that A-MA with higher degree of oxidation will consume more amino in NOCC on account of the formation of Schiff base, leading to the reduction of hydrogen bonds, and then changing the crystal structure of NOCC and attenuating the peak intensity.

The rheological analysis of SSH was monitored by rheometer. To find a suitable hydrogel for further use, thirty-six hydrogel samples were

chosen to conduct rheological analysis, and results were displayed in Table S2. When A-MA (theoretical oxidation degree was 10%) mixed with NOCC, the gelation time varies with the concentration of A-MA or NOCC. Meanwhile, there were similar changes in the concentrations of NOCC or A-MA. Increased A-MA oxidation reduces the gelation time, making subcutaneous injection difficult. However, when gelation time becomes longer, the antigen contained may be released rapidly. For the above reasons, A-MA (20 mg/mL) with theoretical oxidation degree of 20% and NOCC (20 mg/mL) were chosen to subsequent experiments. Moderate gelation time (191 s) and G' make the hydrogel injectable and release antigen slowly.

Molecular weight of selected A-MA was identified by GPC. Compared with mannan ($M_w = 67.0$ kDa), A-MA with a molecular weight

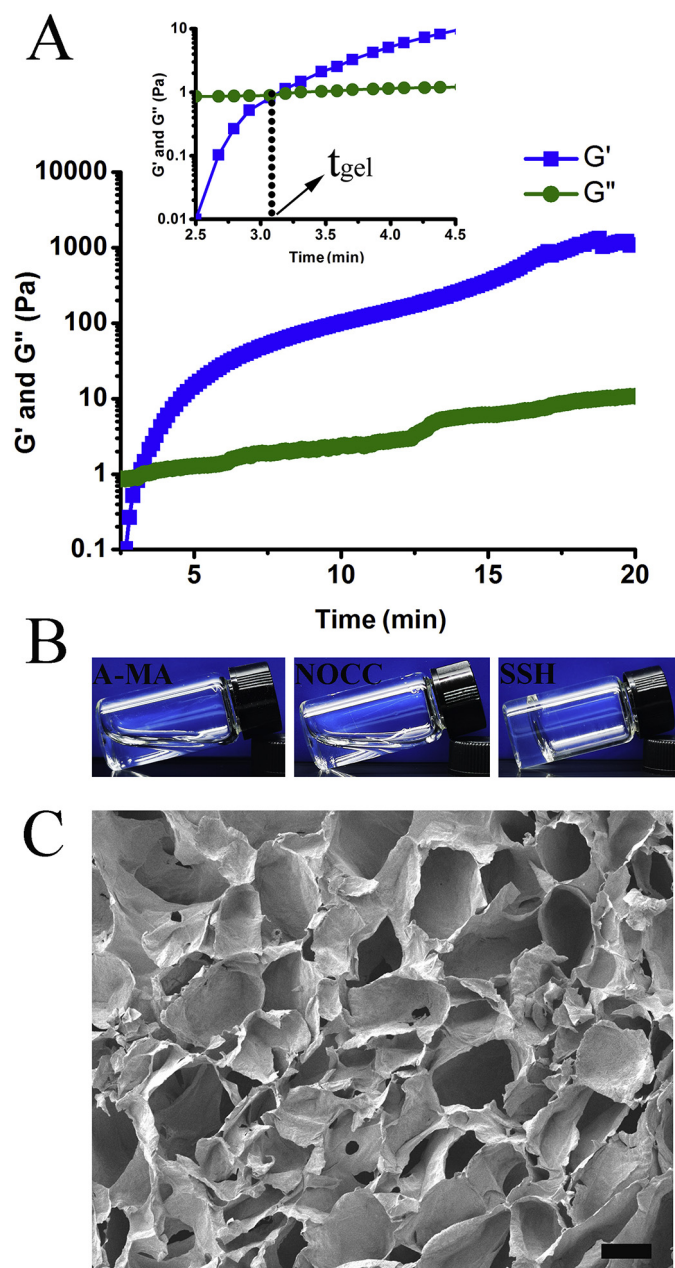


Fig. 2. Rheological analysis, SEM assay and optical image of prepared SSH. (A) The storage modulus (G') and loss modulus (G'') of SSH cross-linked with A-MA (20 mg/mL) and NOCC (20 mg/mL). The crossover time point of G' and G'' curves is the time point of mechanical gel formation (t_{gel}); (B) the optical images of A-MA (20 mg/mL), NOCC (20 mg/mL) and the hydrogel cross-linked with them; (C) SEM image of SSH (scale bar = 100 μm).

of 45.6 kDa had a considerable reduction. Similar to the oxidation of other polysaccharides [22], the decrease of molecular weight may be due to the non-specific oxidation cleaving the glycoside bonds in molecules. The selected hydrogel was characterized rheologically to measure G' and G'' . As shown in Fig. 2A, both of G' and G'' were very low when A-MA mixed with NOCC, while G'' was higher than G' , indicating the sol state of the system. As time went by, A-MA and NOCC were cross-linked due to the formation of Schiff base. Both G' and G'' were increased. Distinctively, G' increased much faster than G'' . Different increasing rates led to the appearance of gelation time (t_{gel}) when $G' > G''$. Subsequently, G' was larger than G'' , indicating the gel state of the system.

Fig. 2B shows the photograph of A-MA (20 mg/mL, w/v), NOCC (20 mg/mL, w/v) and the formed hydrogel. Before gelation, A-MA and NOCC are clear and flowable solution, but the system is a semisolid gel after mixing A-MA and NOCC. A representative SEM image of cross-section of SSH was presented in Fig. 2C. SSH had a continuous and porous structure according to the SEM image, suggesting that SSH may have a high permeability for protein or cells.

The equilibrium swelling rate (ESR) of hydrogel was gravimetrically determined at different pH values of 2, 7.4 and 10, respectively. As shown in Fig. S2, the ESR of SSH depended on the pH value of the solution. In case of high pH (pH = 10), the ESR of hydrogel was 29%, which was 3.5 times higher than that at pH = 2. In neutral or alkaline media, the carboxyl groups in the NOCC ionized gradually and produced a large swelling force through the action of electrostatic repulsion. The carboxyl group forms a hydrogen bond with the hydroxyl group in the acidic media and the amino groups in NOCC is consumed by the aldehyde group in A-MA. Therefore, the protonation of the excess amino

acid cannot form a large electrostatic repulsion, resulting in a weak swelling force.

The porosity of the prepared hydrogel was $58.3 \pm 2.1\%$, which reflected the porous structure of the hydrogel. The large porosity was also consistent with the image observed by SEM.

2.2. Cytotoxicity of A-MA, NOCC and SSH extracts

Cytotoxicity of A-MA, NOCC and SSH extracts was tested on L929 and NIH-3 T3 by MTT assay. As presented in Fig. 3A, the viability of NIH-3 T3 cells were higher than 80% even after incubation with 2.0 mg/mL NOCC for 48 h, while the cell viability decreased accordingly with an increase of concentration of A-MA, but that was higher than 60% even when the concentration was 2.0 mg/mL. The cell activity of L929 was similar to NIH-3 T3 when incubated with A-MA or NOCC (Fig. 3B). Meanwhile, high cell viability of L929 or NIH-3 T3 cells was shown when incubated with SSH extracts for 48 h (Fig. 3C). Previous publications reported the toxic effect of aldehyde content in the oxidized polymer [31]. In the process of our hydrogel formation, aldehyde groups in A-MA reacted with amino groups in NOCC to form Schiff bases. Lower levels of exposed aldehyde group may explain the low toxicity of SSH extracts. These results suggested our SSH had little toxicity, and was suitable for immunological application.

2.3. SSH facilitated antigen internalized by DCs in vitro

As key type of antigen presenting cells (APCs), DCs play a unique role in inducing antigen-specific immune response. The uptake and location of OVA-FITC loaded SSH by DCs were monitored using flow cytometry

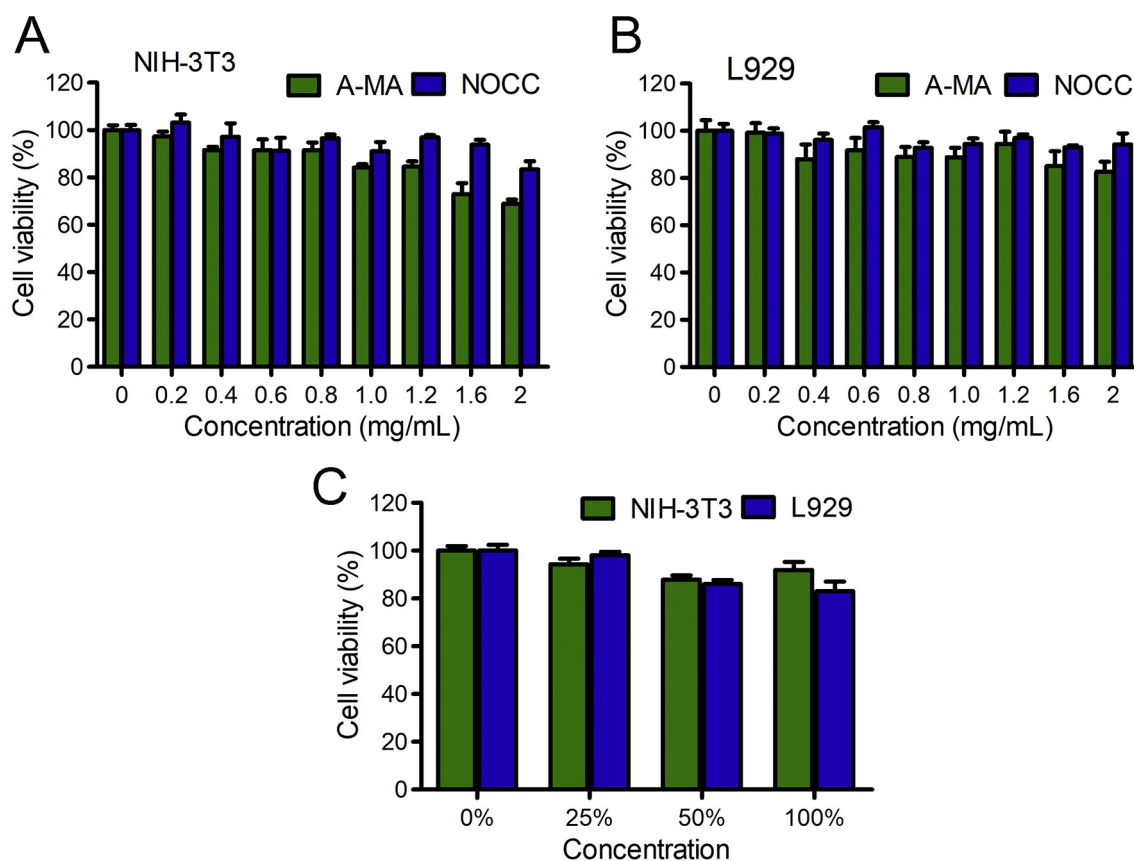


Fig. 3. Cytotoxicity of A-MA, NOCC and SSH extracts. (A) Cell viability of NIH-3 T3 after incubation with A-MA and NOCC for 48 h; (B) Cell viability of L929 after incubation with A-MA or NOCC for 48 h; (C) Cell viability of 3 T3 and L929 after incubation with different concentrations of SSH extracts for 48 h.

and confocal microscope. As shown in Fig. 4A, the percentage of FITC positive DCs in SSH/OVA group was significantly higher than that of DCs cultured with OVA-FITC alone after incubation for 2 and 4 h, suggesting that SSH significantly improved antigen uptake. However, the FITC positive DCs in both groups were few at 4 °C (Fig. 4B), indicating that OVA was taken up by DCs through endocytosis. Then, the intracellular location of antigens by DCs was detected using confocal microscope (Fig. 4C). We observed that green fluorescent (OVA-FITC) colocalized with Lyso-Tracker in DCs from both groups within 4 h of incubation, indicating that antigens were taken up by DCs. Our results confirmed that incorporating antigens into SSH and continuously releasing antigens from which would therefore facilitate the uptake of antigens by DCs.

2.4. SSH promoted DC maturation *in vitro*

DC maturation also plays an essential role in activation of potent antigen specific immune response. Next, the effect of SSH on DC maturation was evaluated. After treated with SSH/OVA, SSH, Medium and OVA solution for 24 h, DCs activation and maturation were detected using flow cytometry. The expression of CD40, CD80 and CD86 co-stimulatory markers (the expression levels of mature) were significantly up-regulated in the presence of SSH or SSH/OVA, while those markers in the medium or OVA group were similar to that of negative control group (Fig. 5A, B and C). The initiation and polarization of T and B cell responses requires the expression of costimulatory molecules. Unlike traditional hydrogels that require commercial vaccine adjuvants

to stimulate DC maturation, such as CpG-ODN (a toll-like receptor 9 agonist) [32], resiquimod (a toll-like receptor 7/8 agonist) [33] and etc., our SSH can be used as a self-adjuvant to up-regulate the expression of CD40, CD80 and CD86 in DCs. Meanwhile, we found that MHC II positive DC cells increased significantly after incubating with SSH/OVA (Fig. 5D). These results highlighted that SSH/OVA can stimulate DCs to maturation status, and promote DCs present antigen to T cells through MHC II molecules.

In addition to antigen/MHC complex and co-stimulatory signals, cytokines secretion by APCs also play an essential role in promoting the activation of T and B cell immune response. In this study, cytokines secreted by DCs was detected using ELISA kits. As shown in Fig. 5E, compared to OVA alone, the Th2-type cytokine IL-6 secreted by DCs was significant increased after SSH/OVA treatment. The secretion of pro-inflammatory IL-1 β showed similar result (Fig. 5F). SSH based vaccine adjuvant might activate DCs in an inflammatory manner. In addition, TNF- α secreted by DCs after SSH/OVA treatment was 1.9-fold higher than that of OVA alone (Fig. 5G). After SSH treatment, the secretion level of IL-12 also significantly increased (Fig. 5H). IL-12 and TNF- α can not only promote the expansion of DCs, but also amplify the function of CD4⁺ T cells, stabilize the connection between DCs and CD4⁺ T cells, and further regulate other immune cell functions. For instance, they can promote macrophages and NK cells secrete other cytokines in turn to induce the maturation of DCs, thus forming a feedback regulation network. SSH could thus be a self-adjuvant and potentially be applied in the preparation of vaccines against different diseases.

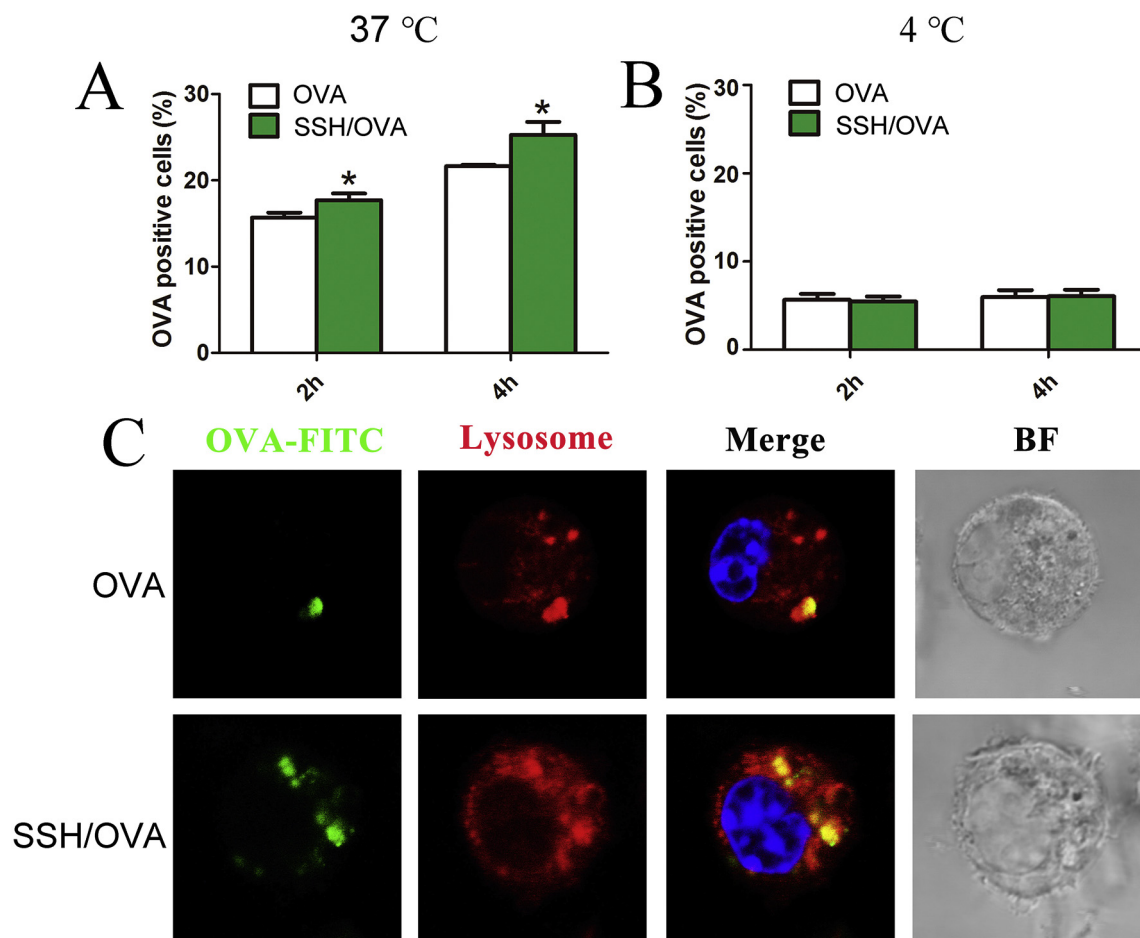


Fig. 4. The effects of SSH on the cellular uptake and intracellular localization of OVA antigen in mouse immature DCs. DCs were incubated with OVA-FITC and SSH loading OVA-FITC at 37 °C (A) and 4 °C (B) for 2 or 4 h, the ratio of OVA-FITC positive cells was measured by flow cytometry. (C) OVA-FITC and SSH loading OVA-FITC were incubated with DCs at 37 °C for 4 h, and the intracellular localization of the antigen was observed by confocal laser scanning microscopy. (* $p < 0.05$).

2.5. In vivo degradation and antigen depot effect of SSH

To assess the degradation of SSH, which was a key index for biomaterials applied in vivo, SSH was subcutaneous injected into the backs of

BALB/c mice. On gross observation, the gel precursor solution rapidly formed hydrogel in situ, and then the hydrogel became smaller and smaller with time (Fig. 6A). The volume of hydrogel was significantly reduced on day 10, and only a few were observed on day 60, and eventually

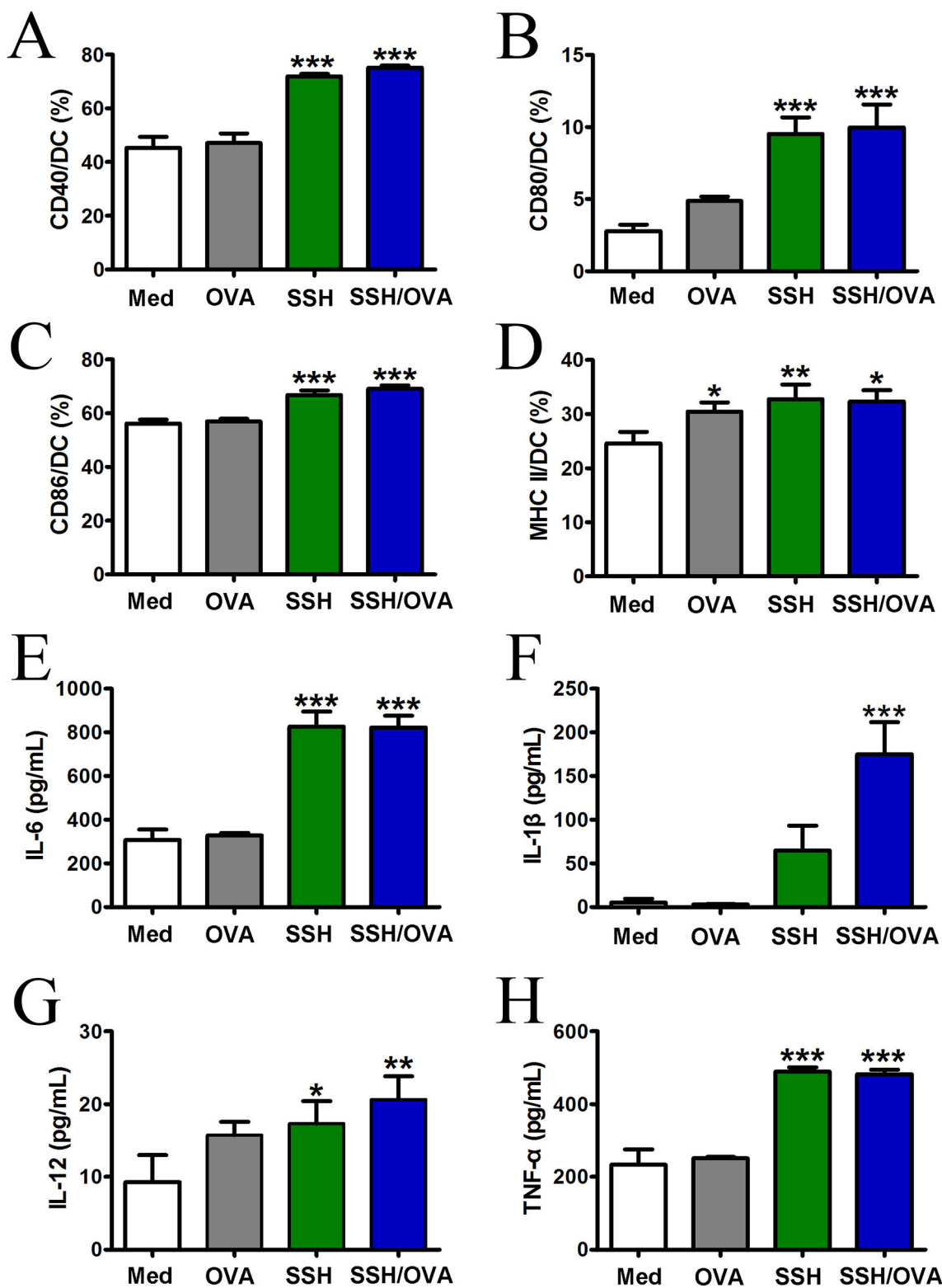


Fig. 5. Expression of the co-stimulatory molecules and MHC II on DCs stimulated with SSH. The expression of CD40, CD80, CD86 and MHC II on DCs were detected by flow cytometry after incubation with OVA, SSH and SSH/OVA for 24 h. Percentages of CD40⁺ (A), CD80⁺ (B), CD86⁺ (C), MHC II⁺ (D) cells were analyzed and the concentration of cytokines in culture supernatants of IL-6 (E), IL-1β (F), IL-12 (G) and TNF-α (H) were measured by ELISA. (**p* < 0.05, ***p* < 0.01 and ****p* < 0.001 indicates the differences between each group and Med group).

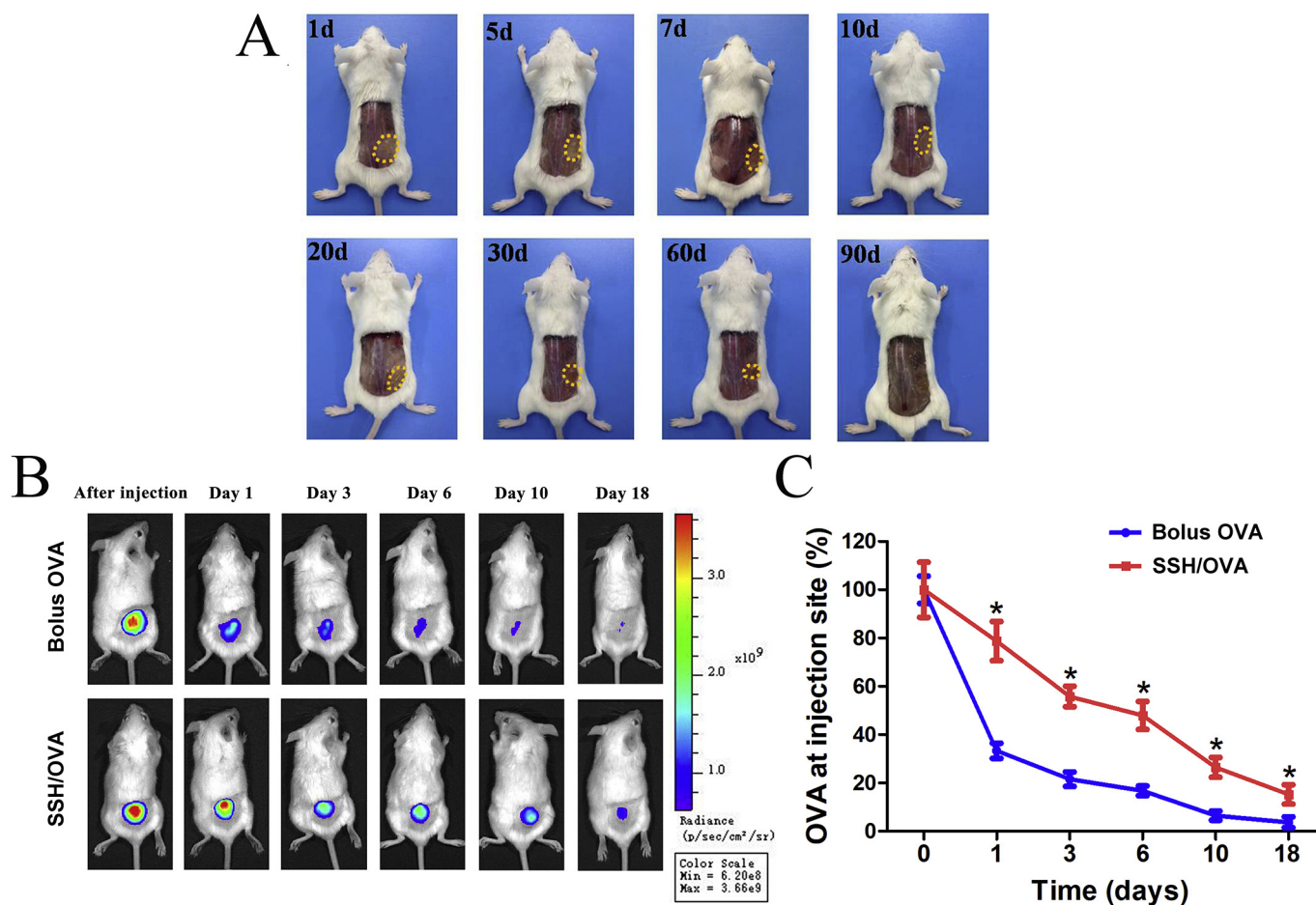


Fig. 6. In vivo degradation and antigen depot effect of SSH. (A) BALB/c mice were subcutaneous immunized with an injection of the same amount of OVA-FITC in PBS or SSH ($n = 3$ animals per condition). Fluorescence images were acquired using an IVIS® Spectrum system. (B) Representative fluorescence images at determined time points for each group. (C) Relative OVA-FITC remaining in injection sites as a function of time, as based on fluorescent imaging (* $p < 0.05$, ** $p < 0.01$, *** $p < 0.001$).

disappeared on day 90. In addition, the histopathologic examination was performed to assess microscopic changes of the tissue surrounding the injection site. As shown in Fig. S3, there were lots of granulocytes infiltrated into the injection site at the first 5 days, but it decreased significantly on the 10th day, and disappeared on day 90 with the degradation of SSH. Besides, there were no hemorrhage or inflammatory exudates observed throughout the observation period. Mice do not carry any associated enzymes to promote subcutaneous enzymatic degradation of mannan, while hydrolysis under physiological conditions can only occur slowly. This may be the reason of long degradation time of SSH.

To investigate the release of OVA from SSH in vivo, OVA was labeled with rhodamin B isothiocyanate (RBITC) and imaged at each time points using fluorescent imaging. The representative fluorescence images are shown in Figure 6B, while Fig. 6C shows the in vivo release curve of OVA calculated with initial fluorescence intensity as total amount. Only $33.31 \pm 3.15\%$ of the initial fluorescence remained one day after injection of bolus OVA (OVA-RBITC in PBS). Meanwhile, the fluorescence had $78.73 \pm 3.15\%$ remaining in SSH/OVA group (OVA-RBITC loaded in SSH). Over this time course, the fluorescence in SSH/OVA group decreased slowly, and was still 4.1-fold higher in SSH/OVA than in the bolus OVA on day 18. These data indicate that SSH might serve as an antigen depot, with extending the in situ release of antigen compared to release of free antigen in PBS. This sustained release of antigen is thought to boost the immune response. For example, phospholipid-based vaccine delivery depot released antigens continuously for nearly one month, which significantly increased the production of antigen-specific antibodies [34]. In another report, antigen specific antibody

response induced by a colloidal vesicle based vaccine depot lasted at least 24 weeks [35]. The vaccine depots can stimulate immune response through the sustained release of antigens. In our research, the SSH has the ability to stimulate the maturation of DCs and promote the production of cytokines. Therefore, SSH is expected to serve as both an antigen delivery vehicle and immunostimulatory agent to boost antigen-specific immune response in vivo.

2.6. SSH increased the accumulation of antigen in lymph nodes

After ingest exogenous antigens, APCs will migrate to lymph nodes where they interact with T cells, thereby inducing an antigen specific adaptive immune response. The ability of SSH to efficiently facilitate the DCs uptake of antigens and maturation prompted us to investigate the effects of SSH on antigen accumulation in lymph node. As presented in Fig. 7A, no fluorescence signal was detected in lymph nodes of control mice after 24 h of injection, while strong fluorescence signals were detected in other groups in both of the proximal and distal lymph nodes. The fluorescence of the proximal lymph nodes in the SSH/OVA group was 3.5-fold and 4.4-fold higher than that in the OVA and Alum/OVA groups, respectively (Fig. 7B). In addition, similar result was found in the distal lymph nodes (Fig. 7B). After 48 h, the fluorescence signal became weaker in all groups (Fig. 7C). However, the signal at the proximal lymph nodes in the SSH group was significantly higher than that in the OVA group ($p = 0.0133$) (Fig. 7D), and stronger fluorescence signal was detected at the distal site in SSH/OVA group compared to the Alum/OVA group (Fig. 7D). Unlike other delivery vehicles that promote antigen

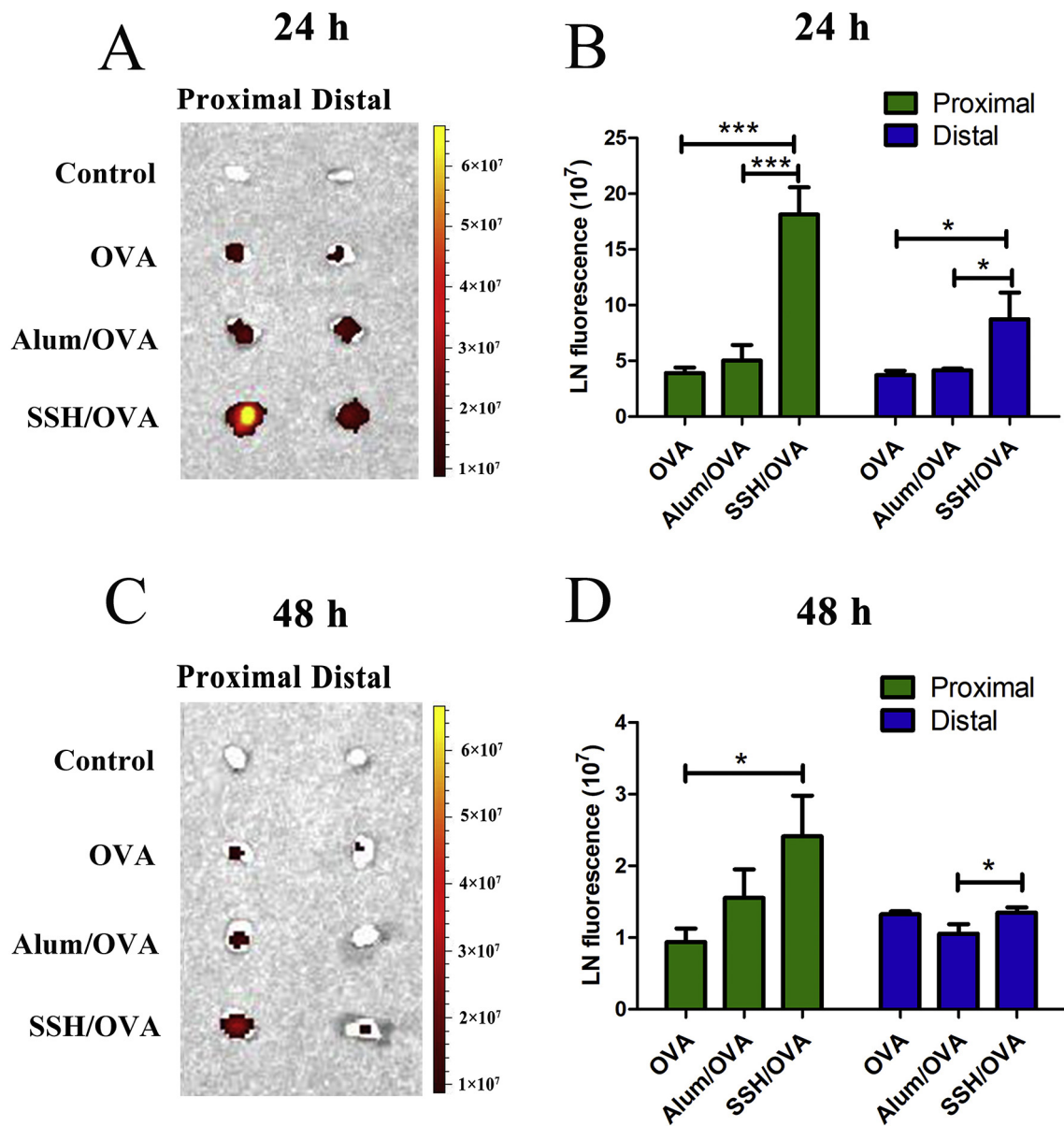


Fig. 7. The effect of SSH on OVA aggregation in lymph nodes. The proximal and distal lymph nodes were obtained and subjected to fluorescence imaging after injected with different vaccine formulations for 24 h (A) and 48 h (C). Proximal represents the lymph node near the injection sites. (B, D) The fluorescence intensity of OVA-RBITC for each lymph node. (* $p < 0.05$, *** $p < 0.001$, ns: not significant).

accumulate in lymph nodes by targeting lymph nodes, our SSH may achieve similar effects by sustainable release and protecting the antigen from rapid degeneration in the body. These results suggested that SSH increased the accumulation of antigen in lymph nodes. Long duration of antigens in lymph nodes provides more possibilities for evoking effective antigen-specific immune response.

2.7. SSH promoted production of antigen-specific antibodies in mice

Antibody titer is a key parameter for evaluating the efficacy of vaccine. The vaccine potency tests of OVA-loaded SSH were conducted in mice. We vaccinated mice with OVA, OVA-absorbed Alum and OVA-loaded SSH, and performed ELISA analysis on 21, 28, 35 and 42 days after priming immunization to measure the total IgG against OVA. As shown in Fig. 8A, IgG titers of SSH group were significantly higher than soluble OVA and Alum/OVA group on day 21. After one week post second booster immunization (on day 28), the titers of SSH/OVA group reached the highest value

compared to other groups. At this time point, SSH increased IgG production by 2500-fold compared with free OVA group, and 12.5-fold compared with Alum/OVA group. On day 35 and 42, titers of SSH/OVA and Alum/OVA group were decreasing, but titers induced by SSH/OVA still significantly higher than that of other groups.

We also measured subtype IgG1 and IgG2b levels to determine the effects of each formulation on Th2 and Th1 cell polarization. As shown in Fig. 8B and C, anti-OVA IgG1 and IgG2b titers were significantly higher in SSH/OVA compared with free OVA and Alum/OVA. Consistent with our results on promoting the production of specific cytokines by DCs, SSH elicited a mixed Th1 and Th2 immune response. Importantly, a bias to IgG1 titers and lower IgG2b titers was observed in SSH/OVA group (Fig. 8B and C), which was similar to Alum group that was supposed to induce a strong humoral (Th2-type) immune response. These data indicated that the SSH augmented humoral immune response compared with free OVA or Alum/OVA, which might be due to its antigen depot effect and capability to induce DCs activation and maturation.

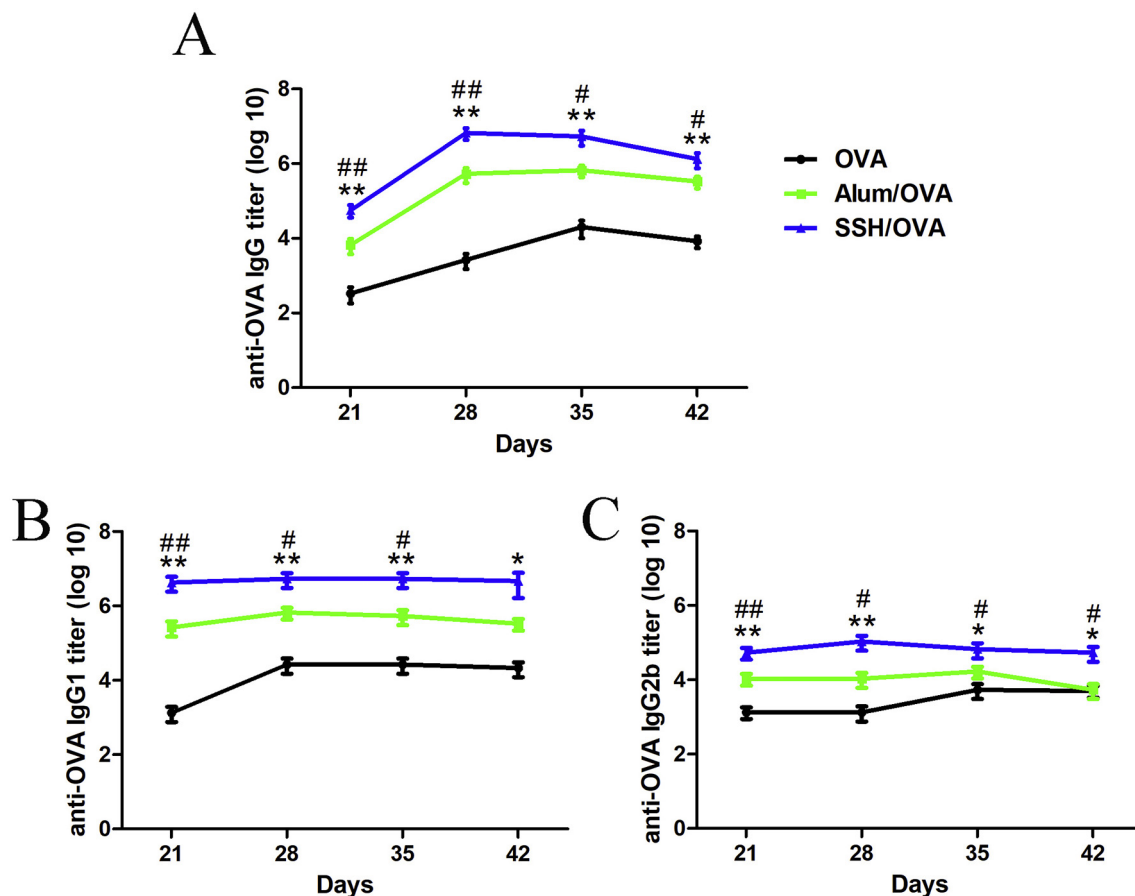


Fig. 8. SSH promoted the production of antigen-specific antibodies in humoral immunity. The detection of antigen-specific antibody in each group over time: (A) IgG, (B) IgG1, (C) IgG2b. The asterisks indicate the difference between the SSH/OVA group and OVA group. * $p < 0.05$, ** $p < 0.01$; the hashtag symbol indicates that differences between SSH/OVA group and Alum group. # $p < 0.5$, ## $p < 0.5$.

2.8. Therapeutic efficacy and safety evaluation of SSH-based vaccines

To determine whether this approach has a therapeutic capability, we treated B16-OVA tumor bearing mice with SSH vaccine. After three therapeutic immunizations, the SSH vaccine delayed the average tumor growth (Fig. S4). In contrast, mice treated with OVA alone or with Alum/OVA had no effect. These results of antigen depot effects, long duration of antigens in lymph nodes, improved antigen uptake and DCs maturation and stronger antibody production highlight the potential of SSH-based vaccines for vaccination strategies. Meanwhile, the body weight of all monitored groups was consistent with only slight changes (Fig. S5), suggesting low or acceptable toxicity of SSH. It is worth noting that aluminum salts are still widely used clinically as vaccine adjuvants, but their toxicity and degradability *in vivo* have attracted extensive attention. Previous studies have shown that aluminum salts are not readily biodegradable in the body and are prone to side effects such as granulomatous inflammation [36], delayed hypersensitivity [37] and etc. SSH is composed of natural polysaccharides that have been simply modified, and we have not observed the obvious toxicity. Nevertheless, we are planning to conduct further safety evaluations of SSH for short-term and long-term *in vivo* applications.

3. Conclusions

In summary, we reported an injectable SSH with biodegradability and low toxicity. SSH can be formed spontaneously *in situ* by Schiff base without additional crosslinking initiators. Further study

suggested that it efficiently facilitated the uptake of antigen by DCs and stimulated DCs activation and maturation, released antigen in a sustained manner, as well as increased the accumulation of antigens in lymph nodes. Furthermore, OVA-loaded SSH induced stronger antigen-specific humoral immune response compared with aluminum adjuvant. Our results indicate that SSH based vaccines can improve the immune response in mice which is one of the few reports that hydrogels can be functioned as both immunostimulatory agent and antigen delivery system. The simple fabrication procedure and the ability to evoke effective immune response suggest the potential application of SSH for immunotherapy.

Author disclosure

The authors declare no conflict of interest.

Data availability

The raw/processed data required to reproduce these findings cannot be shared at this time due to technical or time limitations.

Declaration of Competing Interest

The authors declare that they have no known competing financial interests or personal relationships that could have appeared to influence the work reported in this paper.

Acknowledgments

This work was financially supported by the National Natural Science Foundation of China (No. 81771967 and No. 81822025), the 1·3·5 Project for Disciplines of Excellence, West China Hospital, Sichuan University (ZYQC08002), and the National Program for Support of Top-notch Young Professionals (W02070141).

Appendix A. Supplementary data

Supplementary data to this article can be found online at <https://doi.org/10.1016/j.matdes.2020.109232>.

References

- [1] L. Du, W. Tai, Y. Yang, G. Zhao, Q. Zhu, S. Sun, C. Liu, X. Tao, C.-T.K. Tseng, S. Perlman, S. Jiang, Y. Zhou, F. Li, Introduction of neutralizing immunogenicity index to the rational design of MERS coronavirus subunit vaccines, *Nat. Commun.* 7 (2016) 13473, <https://doi.org/10.1038/ncomms13473>.
- [2] A. Cassone, Development of vaccines for *Candida albicans*: fighting a skilled transformer, *Nat. Rev. Microbiol.* 11 (2013) 884–891, <https://doi.org/10.1038/nrmicro3156>.
- [3] G. Zhu, G.M. Lynn, O. Jacobson, K. Chen, Y. Liu, H. Zhang, Y. Ma, F. Zhang, R. Tian, Q. Ni, S. Cheng, Z. Wang, N. Lu, B.C. Yung, Z. Wang, L. Lang, X. Fu, A. Jin, I.D. Weiss, H. Vishwasrao, G. Niu, H. Shroff, D.M. Klinman, R.A. Seder, X. Chen, Albumin/vaccine nanocomplexes that assemble in vivo for combination cancer immunotherapy, *Nat. Commun.* 8 (2017) 1954, <https://doi.org/10.1038/s41467-017-02191-y>.
- [4] C.B. Rodell, S.P. Arlauckas, M.F. Cuccarese, C.S. Garris, R. Li, M.S. Ahmed, R.H. Kohler, M.J. Pittet, R. Weissleder, TLR7/8-agonist-loaded nanoparticles promote the polarization of tumour-associated macrophages to enhance cancer immunotherapy, *Nat. Biomed. Eng.* 2 (2018) 578–588, <https://doi.org/10.1038/s41551-018-0236-8>.
- [5] D. Shae, K.W. Becker, P. Christov, D.S. Yun, A.K.R. Lytton-Jean, S. Sevimli, M. Ascano, M. Kelley, D.B. Johnson, J.M. Balko, J.T. Wilson, Endosomolytic polymersomes increase the activity of cyclic dinucleotide STING agonists to enhance cancer immunotherapy, *Nat. Nanotechnol.* 14 (2019) 269–278, <https://doi.org/10.1038/s41565-018-0342-5>.
- [6] Y. Wang, X. Wang, J. Zhang, L. Wang, C. Ou, Y. Shu, Q. Wu, G. Ma, C. Gong, Gambogic acid-encapsulated polymeric micelles improved therapeutic effects on pancreatic cancer, *Chin. Chem. Lett.* 30 (2019) 885–888, <https://doi.org/10.1016/j.ccl.2019.02.018>.
- [7] A. Ewald, B. Lochner, U. Gbureck, J. Groll, R. Krüger, Structural optimization of macroporous magnesium phosphate scaffolds and their Cytocompatibility, *Key Eng. Mater.* 493–494 (2011) 813–819, <https://doi.org/10.4028/www.scientific.net/KEM.493-494.813>.
- [8] M. Ashuri, F. Moztafzadeh, N. Nezafati, A. Ansari Hamedani, M. Tahriri, Development of a composite based on hydroxyapatite and magnesium and zinc-containing sol-gel-derived bioactive glass for bone substitute applications, *Mater. Sci. Eng. C* 32 (2012) 2330–2339, <https://doi.org/10.1016/j.msec.2012.07.004>.
- [9] H. Shi, C. Gong, H. Zhang, Y. Wang, J. Zhang, Z. Luo, Z. Qian, Y. Wei, L. Yang, Novel vaccine adjuvant LPS-hydrogel for truncated basic fibroblast growth factor to induce antitumor immunity, *Carbohydr. Polym.* 89 (2012) 1101–1109, <https://doi.org/10.1016/j.carbpol.2012.03.073>.
- [10] B.N. Lambrecht, M. Kool, M.A. Willart, H. Hammad, Mechanism of action of clinically approved adjuvants, *Curr. Opin. Immunol.* 21 (2009) 23–29, <https://doi.org/10.1016/j.coi.2009.01.004>.
- [11] A. Pasquale, S. Preiss, F. Silva, N. Garçon, Vaccine adjuvants: from 1920 to 2015 and beyond, *Vaccines* 3 (2015) 320–343, <https://doi.org/10.3390/vaccines3020320>.
- [12] S.R. Van Tomme, G. Storm, W.E. Hennink, In situ gelling hydrogels for pharmaceutical and biomedical applications, *Int. J. Pharm.* 355 (2008) 1–18, <https://doi.org/10.1016/j.ijpharm.2008.01.057>.
- [13] C.G. Park, C.A. Hartl, D. Schmid, E.M. Carmona, H.-J. Kim, M.S. Goldberg, Extended release of perioperative immunotherapy prevents tumor recurrence and eliminates metastases, *Sci. Transl. Med.* 10 (2018) <https://doi.org/10.1126/scitranslmed.aar1916> eaar1916.
- [14] L. Li, K. Zhang, T. Wang, P. Wang, B. Xue, Y. Cao, L. Zhu, Q. Jiang, Biofabrication of a biomimetic supramolecular-polymer double network hydrogel for cartilage regeneration, *Mater. Des.* 189 (2020) 108492, <https://doi.org/10.1016/j.matdes.2020.108492>.
- [15] E.J. Lee, E. Kang, S.-W. Kang, K.M. Huh, Thermo-irreversible glycol chitosan/hyaluronic acid blend hydrogel for injectable tissue engineering, *Carbohydr. Polym.* 244 (2020) 116432, <https://doi.org/10.1016/j.carbpol.2020.116432>.
- [16] A.A. Shefa, T. Sultana, M.K. Park, S.Y. Lee, J.-G. Gwon, B.-T. Lee, Curcumin incorporation into an oxidized cellulose nanofiber-polyvinyl alcohol hydrogel system promotes wound healing, *Mater. Des.* 186 (2020) 108313, <https://doi.org/10.1016/j.matdes.2019.108313>.
- [17] B. Wang, S. Van Herck, Y. Chen, X. Bai, Z. Zhong, K. Deswarte, B.N. Lambrecht, N.N. Sanders, S. Lienenklaus, H.W. Scheeren, S.A. David, F. Kiessling, T. Lammers, B.G. De Geest, Y. Shi, Potent and prolonged innate immune activation by enzyme-responsive imidazoquinoline TLR7/8 agonist prodrug vesicles, *J. Am. Chem. Soc.* (2020) <https://doi.org/10.1021/jacs.0c01928> (jacs.0c01928).
- [18] S.G. Reed, M.T. Orr, C.B. Fox, Key roles of adjuvants in modern vaccines, *Nat. Med.* 19 (2013) 1597–1608, <https://doi.org/10.1038/nm.3409>.
- [19] G. Della Giustina, A. Gandin, L. Brigo, T. Panciera, S. Giulitti, P. Sgarbossa, D. D'Alessandro, L. Trombi, S. Danti, G. Brusatin, Polysaccharide hydrogels for multiscale 3D printing of pullulan scaffolds, *Mater. Des.* 165 (2019) 107566, <https://doi.org/10.1016/j.matdes.2018.107566>.
- [20] T. Zhu, J. Mao, Y. Cheng, H. Liu, L. Lv, M. Ge, S. Li, J. Huang, Z. Chen, H. Li, L. Yang, Y. Lai, Recent progress of polysaccharide-based hydrogel interfaces for wound healing and tissue engineering, *Adv. Mater. Interfaces* 6 (2019) 1900761, <https://doi.org/10.1002/admi.201900761>.
- [21] A.O. Tzianabos, Polysaccharide immunomodulators as therapeutic agents: structural aspects and biologic function, *Clin. Microbiol. Rev.* 13 (2000) 523–533, <https://doi.org/10.1128/CMR.13.4.523-533.2000>.
- [22] H. Yu, J. Lu, C. Xiao, Preparation and properties of novel hydrogels from oxidized Konjac Glucomannan cross-linked chitosan for in vitro drug delivery, *Macromol. Biosci.* 7 (2007) 1100–1111, <https://doi.org/10.1002/mabi.200700035>.
- [23] U. Gazi, L. Martinez-Pomares, Influence of the mannose receptor in host immune responses, *Immunobiology.* 214 (2009) 554–561, <https://doi.org/10.1016/j.imbio.2008.11.004>.
- [24] K.L. White, T. Rades, R.H. Furneaux, P.C. Tyler, S. Hook, Mannosylated liposomes as antigen delivery vehicles for targeting to dendritic cells, *J. Pharm. Pharmacol.* 58 (2006) 729–737, <https://doi.org/10.1211/jpp.58.6.0003>.
- [25] R. Mathiesen, H.M.S. Eld, J. Sørensen, E. Fuglsang, L.D. Lund, V. Taverniti, H. Frøkiær, Mannan enhances IL-12 production by increasing bacterial uptake and endosomal degradation in *L. acidophilus* and *S. aureus* stimulated dendritic cells, *Front. Immunol.* 10 (2019) <https://doi.org/10.3389/fimmu.2019.02646>.
- [26] V. Tseveleki, T. Tselios, I. Kanistras, O. Koutsoni, M. Karamita, S.-S. Vamvakas, V. Apostolopoulos, E. Dotsika, J. Matsoukas, H. Lassmann, L. Probert, Mannan-conjugated myelin peptides prime non-pathogenic Th1 and Th17 cells and ameliorate experimental autoimmune encephalomyelitis, *Exp. Neurol.* 267 (2015) 254–267, <https://doi.org/10.1016/j.expneurol.2014.10.019>.
- [27] S.A. Ayati Najafabadi, H. Keshvari, Y. Ganji, M. Tahriri, M. Ashuri, Chitosan/heparin surface modified polyacrylic acid grafted polyurethane film by two step plasma treatment, *Surf. Eng.* 28 (2012) 710–714, <https://doi.org/10.1179/1743294412Y.0000000037>.
- [28] N.S. Ibrahim, G. Krishnamurthy, H. Rao Balaji Raghavendran, S. Puvanewary, N. Wuey Min, T. Kamarul, Novel HA-PVA/NOCC bilayered scaffold for osteochondral tissue-engineering applications – Fabrication, characterization, in vitro and in vivo biocompatibility study, *Mater. Lett.* 113 (2013) 25–29, <https://doi.org/10.1016/j.matlet.2013.09.026>.
- [29] S.-Y. Lee, A.-S. Wee, C.-K. Lim, A.A. Abbas, L. Selvaratnam, A.M. Merican, T.S. Ahmad, T. Kamarul, Supermacroporous poly(vinyl alcohol)-carboxylmethyl chitosan-poly(ethylene glycol) scaffold: an in vitro and in vivo pre-assessments for cartilage tissue engineering, *J. Mater. Sci. Mater. Med.* 24 (2013) 1561–1570, <https://doi.org/10.1007/s10856-013-4907-4>.
- [30] L. Li, N. Wang, X. Jin, R. Deng, S. Nie, L. Sun, Q. Wu, Y. Wei, C. Gong, Biodegradable and injectable in situ cross-linking chitosan-hyaluronic acid based hydrogels for postoperative adhesion prevention, *Biomaterials.* 35 (2014) 3903–3917, <https://doi.org/10.1016/j.biomaterials.2014.01.050>.
- [31] M. Sokolsky-Papkov, A.J. Domb, J. Golenser, Impact of aldehyde content on amphotericin B–dextran imine conjugate toxicity, *Biomacromolecules.* 7 (2006) 1529–1535, <https://doi.org/10.1021/bm050747n>.
- [32] X. Yang, C. Lai, A. Liu, X. Hou, Z. Tang, F. Mo, S. Yin, X. Lu, Anti-tumor activity of mannose-CpG-Oligodeoxynucleotides-conjugated and Hepatoma lysate-loaded Nanoliposomes for targeting dendritic cells in vivo, *J. Biomed. Nanotechnol.* 15 (2019) 1018–1032, <https://doi.org/10.1166/jbnn.2019.2755>.
- [33] G.M. Lynn, R. Laga, P.A. Darrach, A.S. Ishizuka, A.J. Balaci, A.E. Dulcey, M. Pechar, R. Pola, M.Y. Gerner, A. Yamamoto, C.R. Buechler, K.M. Quinn, M.G. Smelkinson, O. Vanek, R. Cawood, T. Hills, O. Vasalati, K. Kastenmüller, J.R. Francica, L. Stutts, J.K. Tom, K.A. Ryu, A.P. Esser-Kahn, T. Etrych, K.D. Fisher, L.W. Seymour, R.A. Seder, In vivo characterization of the physicochemical properties of polymer-linked TLR agonists that enhance vaccine immunogenicity, *Nat. Biotechnol.* 33 (2015) 1201–1210, <https://doi.org/10.1038/nbt.3371>.
- [34] L. Han, J. Xue, L. Wang, K. Peng, Z. Zhang, T. Gong, X. Sun, An injectable, low-toxicity phospholipid-based phase separation gel that induces strong and persistent immune responses in mice, *Biomaterials.* 105 (2016) 185–194, <https://doi.org/10.1016/j.biomaterials.2016.08.007>.
- [35] R.G. Schaut, M.T. Brewer, K. Mendoza, J. Jackman, B. Narasimhan, D.E. Jones, A polyanhydride-based implantable single dose vaccine platform for long-term immunity, *Vaccine.* 36 (2018) 1024–1025, <https://doi.org/10.1016/j.vaccine.2017.11.067>.
- [36] T. Ono, K. Goto, S. Takagi, S. Iwasaki, H. Komatsu, Sclerosing effect of OC-108, a novel agent for hemorrhoids, is associated with granulomatous inflammation induced by aluminum, *J. Pharmacol. Sci.* 99 (2005) 353–363, <https://doi.org/10.1254/jphs.FP05026X>.
- [37] H.K. Lehman, H.S. Faden, Y.V. Fang, M. Ballow, A case of recurrent sterile abscesses following vaccination: delayed hypersensitivity to aluminum, *J. Pediatr.* 152 (2008) 133–135, <https://doi.org/10.1016/j.jpeds.2007.08.039>.